Pharm Res (2015) 32:445–457
DOI 10.1007/s11095-014-1473-5

RESEARCH PAPER

Characterisation of Skin Barrier Function Using Bioengineering and Biophysical Techniques

Quan Yang • Richard H. Guy

Received: 25 February 2014 / Accepted: 24 July 2014 / Published online: 5 August 2014
© Springer Science+Business Media New York 2014

ABSTRACT

Purpose To characterise skin barrier function *in vivo* at two distinct anatomic sites using minimally invasive bioengineering and biophysical tools.

Methods In healthy human volunteers, the quantities of stratum corneum (SC) per unit area of skin on the forearm and forehead were quantified by gravimetric and imaging techniques. Organisation of the SC intercellular lipids was evaluated as a function of position using attenuated total reflectance infrared spectroscopy (ATR-IR). The constituents of natural moisturising factor (NMF) were extracted from tape-stripped samples of the SC and by reverse iontophoresis; 21 components were identified and quantified by liquid chromatography with mass spectrometric detection.

Results SC was quantified more accurately by imaging and was significantly thinner on the forehead than on the forearm. Intercellular lipids were more disordered near the skin surface at both sites; however, throughout forearm SC, the lipids were substantially better organised than those in the forehead. Compositionally, the NMF from forearm and forehead SC was similar, but the total amount extractable from the forehead was smaller.

Conclusion Taken together, the bioengineering and biophysical techniques employed demonstrate, in a complementary, objective and quantitative fashion, that SC barrier function on the forehead is less competent than that on the forearm.

KEY WORDS infrared spectroscopy · reverse iontophoresis · skin barrier function natural moisturizing factor (NMF) · stratum corneum

Q. Yang • R. H. Guy (✉)
Department of Pharmacy & Pharmacology, University of Bath, Claverton Down, Bath BA2 7AY, UK
e-mail: r.h.guy@bath.ac.uk

Q. Yang
MHRA, 151 Buckingham Palace Road, London SW1W 9SZ, UK

ABBREVIATIONS

AD	Atopic Dermatitis
A_{SC}	SC absorbance
ATR-FTIR	Attenuated total reflectance-Fourier transform infrared spectroscopy
DPK	Dermatopharmacokinetics
G_{SC}	Mean greyscale value of tape onto which SC has been stripped
G_{tape}	Mean greyscale value of a blank tape
l	Thickness of the corneocytes on the tape
LCMS	Liquid chromatography mass spectrometry
M_{SC}	Weight of SC on each tape
NMF	Natural moisturizing factor
PCA	Pyrrolidone carboxylic acid
SC	Stratum corneum
TEWL	Transepidermal water loss
α_{SC}	Absorption coefficient of the SC

INTRODUCTION

Natural moisturizing factor (NMF) is a collection of water-soluble, low molecular weight compounds found in the stratum corneum (SC). Functionally, it allows the SC to retain water against the dehydrating action of external environment and thus plays a key role in skin hydration (1). NMF is composed primarily of free amino acids (AAs) and amino acid derivatives that are derived from filaggrin. Filaggrin is synthesized from profilaggrin, an approximately 500-kDa insoluble protein, consisting of 10 to 12 repeating filaggrin units (2,3). During the transition of the mature granular cell into a corneocyte, rapid dephosphorylation of pro-filaggrin occurs, yielding filaggrin (3). As corneocytes proceed upwards through the SC, deiminiation and complete proteolysis of filaggrin yields the main components of NMF, specifically, (a) free hygroscopic amino acids (mainly Ser, Ala, Arg, Gly,

Pro and His (4)), and (b) the following amino acid derivatives: pyrollidone carboxylic acid (PCA) formed by cyclisation of glutamine (5), trans-urocanic acid (UCA) synthesised from histidine (3), and ornithine (Orn) and citruline (Cit), which are degradation products of arginine (6).

Presently, a filaggrin mutation is considered to be the strongest genetic risk factor for atopic dermatitis (AD) (7–10). As a result of this mutation, lower levels of NMF are generated in atopic skin and this is thought to contribute to an impaired barrier function (4,11). Furthermore, a reduced NMF level has also been reported in other abnormal dry and scaly skin conditions (12–14). Therefore, measuring the amount of NMF in the skin may offer a useful indicator of skin hydration and be helpful in the early diagnosis of these skin disorders. In this study, NMF components have been extracted *in vivo* from forearm and forehead SC (i) following tape-stripping, and (ii) less invasively using reverse iontophoresis (15,16). Absolute quantification of 21 constituents of NMF has been possible with a sensitive liquid chromatography – mass spectroscopic assay.

Regional skin differences at various anatomical sites have been recognised (17,18). For example, the SC on the face is thinner, and contains smaller corneocytes than that on the forearm. The surface area of facial corneocytes is smaller, resulting in a shorter path-length for molecular transport and a noticeably higher permeability (19,20). In addition, the face is one of the first body sites affected when atopic dermatitis (AD) develops and the ratio of fragile to mature corneocytes is higher here than on the inner upper arm (21). Voegeli et al (22) have also demonstrated higher levels of desquamation-related proteases on the face. All these features are found in AD and it was highlighted, therefore, that the forearm and forehead skin of healthy volunteers might model the distinction between a competent SC and one pre-predisposed to AD.

The goal of this project, then, was to apply selected bioengineering and biophysical techniques to evaluate skin barrier function on the forehead and forearm and to identify regional differences in barrier thickness, SC lipid arrangement and NMF quantity and composition. To examine these properties of the SC, from the skin surface to the interface with the stratum granulosum, repeated tape-stripping has been used. In the literature, the amount of SC removed (and the depth into the barrier) has been primarily assessed either gravimetrically or by the evaluation of protein content. Recently a novel imaging technique (23–25) has been validated against these standard approaches and its use in the current study has again demonstrated its value in terms of speed and efficiency. NMF components have been quantified in the SC tape-strips and less invasively following their extraction by reverse iontophoresis (15,16). In parallel, SC lipid amount and conformational order has been determined by infrared spectroscopy (26). Taken together, the results obtained have provided a comprehensive picture of skin barrier function *in vivo* in man at two distinct anatomic sites, the forearm and the forehead.

MATERIALS AND METHODS

Chemicals

Sodium azide, NFPA (perfluoropentanoic acid), silver (Ag) wire (>99.99% purity), AgCl (99.999%), acetonitrile and all L-amino acids (Asn, Ser, Gly, Asp, Cit, Orn, Gln, Glu, Thr, Ala, Pro, Val, Tyr, Met, Ile, Leu, His, Lys, Phe, Arg, and Trp) were purchased from Sigma-Aldrich Co. (Gillingham, UK). Glycine-D5, Serine-D3, Glutamine-D5 were purchased from Cambridge Isotope Laboratories (Andover,MA). Deionised water (resistivity ≥18.2 MΩ/cm^2) was used to prepare all aqueous solutions (Barnstead Nanopure Diamond™, Dubuque, IA).

Study Design

Ethical approval was granted by the University of Bath Research Ethics Committee for Health and informed consent was obtained from all subjects. No volunteers had any history of dermatological disease, and restrained from using topical formulations prior to the study. A total of 18 volunteers (9 male, 9 female; age range 20–42 years) participated in the experiments described either as a group of 12, or as a group of 6.

Experiments were performed on three separate occasions, at least four weeks apart, on blemish-free sites of the ventral forearm and forehead that were first wiped clean with an isopropyl alcohol swab (Medi-Swab, Seton Healthcare Group plc, England). The three experiments involved: (a) Passive and reverse iontophoretic extraction (and subsequent characterisation) of NMF from the skin over periods of 4 and 3 h, respectively. (b) Tape-stripping repeatedly to remove a significant fraction of the barrier, followed by extraction and analysis of NMF constituents in the SC samples. (c) Sequential tape-stripping of the SC once again with interspersed attenuated total reflectance infrared spectroscopic (ATR-IR) measurements on the newly exposed surface of the skin. The specific experimental details are now presented.

Tape-Stripping

Tape-stripping progressively ablated the stratum corneum (SC) by the repeated application and removal of either D-Squame® disks or Permacel J-LAR® tape. The former were used only on the ventral forearm and were applied to the skin under 225 g/cm^2 of pressure for 5 s; the device for applying pressure was supplied by the D-Squame® manufacturer. The latter was used on both the forearm and the forehead. In this

case, a template with a central square hole (2×2 cm^2) was first fixed to the skin with self-adhesive medical tape (Curafix H, Lohmann & Rauscher, Rengsdorf, Germany) to ensure that all tape-strips were taken from exactly the same site. The tapes (2.5×3 cm^2) were applied with pressure from a weighted roller and then swiftly removed. Transepidermal water loss (TEWL) measurements were taken (AquaFlux V4.7, Biox Systems Ltd., London, UK) before and after each tape strip; the procedure was stopped when TEWL reached 3-4 times the initial value, at which point approximately 75% of the SC had been removed (27).

Passive Diffusion Extraction

A glass cell (internal diameter 1.55 cm, extraction surface 1.89 cm^2) was adhered to either the ventral forearm or the forehead of the subjects using silicone grease and medical grade tape (Curafix H, Lohmann & Rauscher, Rengsdorf, Germany) and was filled with 1 ml of 20 mM ammonium chloride in 10 mM ammonium bicarbonate buffer at pH~ 6.8. Samples were collected at 30 min and at 1 h of passive extraction and then every hour thereafter for a total of 4 h. The collected samples were passed through a sterile syringe filter (Cronus, 0.45 μm, 4 mm diameter, SMI-LabHut Ltd, Gloucester, UK) and stored in the freezer at -20°C until analysis.

Reverse Iontophoretic Extraction

Two glass cells (internal diameter 1.55 cm, extraction surface 1.89 cm^2) separated by ~4 cm were fixed to the skin as before and both were filled with 1 ml of the same extraction solution as that used in the passive experiments above. A direct current of 0.4 mA (i.e., 0.21 mA/cm^2) was applied from a Phoresor II Auto (Iomed, Model No. PM850, Salt lake City, UT) via Ag/AgCl electrodes. The entire contents of the anode and cathode chambers were collected and replaced by an equal volume of extraction solution after 15 and 30 min of iontophoresis and then every half-hour thereafter for a total extraction time of 3 h. Identical sample filtration and storage procedures were followed as described above.

Attenuated Total Reflectance - Infrared Spectroscopy (ATR-FTIR)

Equipment

A PerkinElmer Spectrum 100 Fourier transform IR spectrometer (Waltham, MA, USA), equipped with a universal ATR accessory (single bounce top-plate) with a round diamond crystal (2 mm diameter), was used.

Experiments

Before any measurement, the skin site (either forearm or forehead) was cleaned with a gentle alcohol wipe (Medi-Swab, Seton Healthcare Group plc, London, U.K.). Three IR spectra with 16 scans each were then recorded. The SC was progressively removed by the repeated application and removal of adhesive tape-strips as outlined above. On the forearm, 3 replicate IR spectra were recorded after removal of each tape for the first 6 strips and after every two tapes thereafter. On the forehead, 3 replicate spectra were recorded after each tape-strip.

Spectral Analysis

FTIR spectra were collected in the frequency range 4000-400 cm^{-1}. The peak frequencies of the asymmetric (~2920 cm^{-1}) and symmetric (~2850 cm^{-1}) CH_2 stretching absorbances were obtained from the first-order derivative of the spectra using the Spectrum™ Express software. The normalised areas under the CH_2 stretching absorbances were calculated as previously described (28).

Analysis of Tapes

Infrared Densitometry

The pseudo-absorption of SC protein on the D-Squame® disks was determined using an infrared densitometer (SquameScan TM 850A®, Heiland Electronic, Wetzlar, Germany). The disks were placed into a well, adhesive side up, exposing the measured area (1.8 cm^2, i.e., about 45% of the disk). Prior to the experiment, the instrument was calibrated against a blank sample.

Gravimetric Method

Tapes were prepared at least 12 h before any experiment. Static electricity was discharged from the tapes prior to weighing (R50 discharging bar and ES50 power supply from Eltex Elektrostatick GmbH, Weil am Rhein, Germany). The tapes were weighed before and after stripping on a 0.1 μg precision balance (Sartorius SE2-F, Epsom, UK) to determine the mass of SC removed. Dividing this mass by the strip area (4 cm^2) and by the SC density (1 g/cm^3), the thickness of the SC layer removed was calculated. Six blank tapes were weighed at the same time as the tapes used for SC stripping to correct for any variations due to environmental or other factors.

Imaging Method

The tapes were also photographed using a Coolscan slide scanner (Nikon UK Limited, Kingston-upon-Thames, U.K.) at a resolution of 4000 pixels per inch (157.5 pixels/mm) according to the method previously described (23,24). A crop of approximately 2×2 cm^2 was centred over each image and then scanned. The resulting images were analysed using ImageJ (Rasband, W.S., U.S. National Institutes of Health, Bethesda, Maryland, USA; freeware from http://rsb.info.nih.gov/ij/) to obtain mean greyscale values. Each image was assigned a greyscale value in the range from 0 to 64608, representing 'black' and 'white', respectively. ImageJ calculated the mean greyscale over all pixels. As a control, the mean greyscale of six blank tapes was determined.

Extraction of NMF Constituents

NMF in the SC removed on the tape-strips was subsequently extracted with an aqueous solution of sodium azide (20 mg/l). The first and second tapes were extracted individually into 0.5 ml of extraction solution, while the remaining tapes were extracted into 1 ml. The extracted solutions were filtered (Cronus, 0.45 µm, 4 mm diameter, SMI-LabHut Ltd, Gloucester, U.K.) and stored at −20°C until analysis.

NMF Analysis

LCMS analysis of the SC extracts was performed on a Shimadzu LCMS-2010EV (Shimadzu Corporation, Kyoto, Japan) with a single quadrupole and a dual ion source (containing both electrospray and atmospheric pressure chemical ionization). The MS was operated in positive ion mode with the ion spray voltage set at 1.5 kV. Nitrogen was used both as a nebulising and drying gas at a flow rate of 1.5 L/min with a heat block temperature of 480°C and curved desolvation line temperature of 230°C. The quadrupole was operated in the selected ion monitoring mode and protonated molecules $[M + H]^+$ were used for quantification (Tau 126, Urea 61, PCA 130, Asn 133, Ser 106, serine-D3 109, Gly 76, Glycine-D5 78, Asp 134, Gln 147, glutamine-D5 152, Glu 148, Thr 120, Ala 90, Cit 176, Pro 116, Met 150, trans-urocanic acid 139, cis-urocanic acid 139, Val 118, Tyr 182,Orn 133, His 156, Lys 147, Ile 132, Leu 132, Arg 175, Phe 166, Try 205).

Separation was carried out on a Gemini C18 column (50× 4.6 mm, 3 µm, 110 Å, Phenomenex, Torrance, CA, USA) at 40°C and a flow-rate of 0.3 ml/min. A gradient was used with eluent A comprising a 20 mM nonafluoropentanoic acid solution and eluent B acetonitrile. The gradient elution started with 99:1 (*v*/*v*) A:B for 5 min, followed by a linear change to 86:14 (*v*/*v*) A:B over 9 min, then 86:14 (*v*/*v*) for 5 min, and subsequently altered linearly to 64:36*v*/*v*) over 14 min. The MS was then switched to negative ion mode with 20/80 (*v*/*v*) A:B for 3 min to wash the column and finally equilibrated for 20 min under initial conditions.

Data Interpretation and Statistics

Linear regression was used in the initial analysis of the "training" SC thickness dataset from the weighing and imaging methods. Amino-acid-derived components of NMF in the SC were expressed in terms of amount per unit mass. The change in TEWL as a function of the amount of SC removed was modelled (29) to obtain SC thickness from both the gravimetric and imaging experiments. Extraction fluxes were calculated by dividing the amounts removed during a sampling interval by the duration of that collection period. Amounts extracted were divided by skin area and expressed in nmol/cm^2. Data manipulation and statistics were performed using Graph Pad Prism v. 5.01 (Graph Pad Software Inc., San Diego, CA, U.S.A.). When datasets were compared, a 1-way ANOVA followed by Bonferroni's multiple comparison test was used and the level of statistical significance was fixed at $P<0.05$. All results were expressed as mean ± SD.

RESULTS

Methods to Quantify SC on Tape-Strips and to Determine SC Thickness

Correlation Between Infrared Densitometry and Imaging

Infrared densitometry measurements of light absorbance and the greyscale values from the imaging method were, as expected, highly linearly correlated; with both parameters expressed in terms of percentage, the slope and intercept were 0.76 and 1.56, respectively, with an r^2 of 0.91 ($n=215$).

Correlation Between Gravimetric and Imaging Methods (Forearm SC)

Recent publications (23,24) have demonstrated that the imaging approach may provide a simpler and more precise method than the traditional gravimetric procedure for SC quantification. Further confirmation of this alternative strategy was obtained in the course of this study. Focussing attention first on the SC stripped from the ventral forearm, a total of 678 samples were available for comparing the two methodologies. Of these, 6 tapes removed more than 0.11 mg/cm^2 of material, an amount considered to be artifactually high and probably the result of unknown surface contamination (all aberrant values being observed on the first tape-strip, in fact). The remaining 672 data points were randomly assigned to a "training" set of 336 and a 'test' set of the same number. For

the "training" set, the SC masses (M_{SC}) removed and determined gravimetrically were then correlated (Fig. 1a) with the corresponding absorbances determined by the imaging method (A_{SC}=-log (G_{SC}/G_{tape}), where G_{SC} and G_{tape} are the mean greyscale values of the tape onto which the SC has been stripped and that of a blank tape, respectively) and the following relationship was derived:

$$M_{SC} = 0.36 \text{ x } A_{SC} + 0.009; r^2 = 0.73 \quad (1)$$

The 95% confidence intervals for the slope and intercept were 0.33–0.38 and 0.007–0.011, respectively. Using Eq. 1, the weight of SC on the 'test' tape-strips were predicted from the mean greyscale values and compared to the experimentally measured SC masses. The agreement was good, with no systematic over- or under-prediction observed (Fig. 1b). The differences between measured and predicted values were approximately normally distributed about zero with more than 90% falling between -0.01 and +0.01 mg/cm^2; the mean prediction error for the entire 'test' set was 0.0012 (±0.013) mg/ cm^2.

Correlation Between Gravimetric and Imaging Methods (Forehead SC)

Figure 2a compares gravimetric and imaging methods to quantify SC removed from the forearm and forehead. The apparent weight of material removed from the forehead (at a particular greyscale value) was consistently greater than that from the forearm, an anomalous outcome given that the SC on the forehead is known to be thinner than that at most other body sites. The latter was further confirmed by the significantly higher baseline TEWL values measured on the forehead (20.2 (±4.8) mg/cm^2/hr) compared to the forearm (11.6 (±2.3) mg/cm^2/hr), and that, on average, 21 tape-strips had to be removed from the forearm to provoke a 3–4 fold increase in TEWL, while only 11 were needed on the forehead. The logical interpretation of this observation is that the copious amount of sebaceous lipids secreted on the forehead are significantly contributing to the apparent SC weight measured gravimetrically but that these lipids are "transparent" to the imaging method.

SC Thickness on the Forearm and Forehead

When the gravimetric and imaging data were used to determine SC thickness (29) on the forearm, there was complete agreement between the values deduced (9.6 (±2.7) μm and 8.9 (±2.5) μm, respectively). In contrast, SC thickness assessed by the imaging method on the forehead (4.5 (±1.0) μm) was approximately 50% of, and significantly less than, that on the forearm (whereas the gravimetric approach found

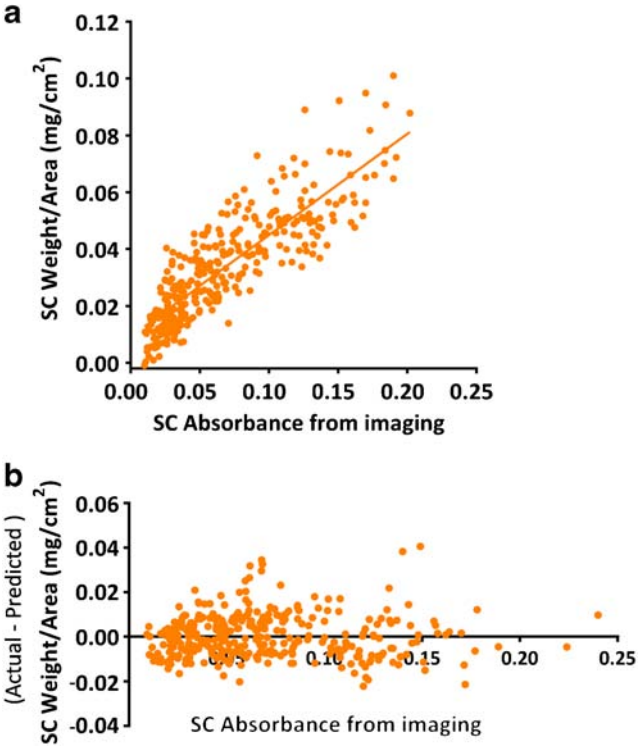

Fig. 1 (**a**) Correlation of SC quantification by gravimetric and imaging methods. The data are from the forearm "training" set described in the text. The linear regression shown corresponds to Eq. (1): $M_{SC} = 0.36 \times A_{SC} + 0.009$; $r^2 = 0.73$. (**b**) Differences between actual and predicted SC weights on the "test" tape-strips ($n = 339$) plotted as a function of SC absorbance determined by the greyscale imaging method.

no difference: 9.4 (±1.9) μm) (Fig. 2b). The surprisingly high apparent SC weights from the forehead (as compared to the forearm: P=0.0015, 2-tailed t-test) were almost completely due to the large quantities on the first two tape-strips (tape 1 from the forehead had, on average, 3 times more than the corresponding tape from the forearm; for tape 2, the difference was a factor of 2), again strongly implicating the substantial presence of sebaceous lipids.

IR Absorbance of Lipids (CH_2 Stretching Absorbance)

IR spectroscopy has been used to report on biomembrane lipid ordering through the CH_2 stretching absorbances from the methylene groups of the lipid acyl chains. The CH_2 stretching absorbance undergoes a blue shift, i.e., a shift to a higher wavenumber, when the degree of lipid disorder increases.

Figure 3a shows that the peak asymmetric (~2920 cm^{-1}) and symmetric (~2850 cm^{-1}) CH_2 stretching absorbances occurred at significantly higher wavenumbers at the skin surface before tape-stripping. This is most probably due to the contribution from sebaceous lipids (28). The CH_2 stretching frequencies at both sites before tape-stripping are significantly higher than those after tape-stripping (repeated

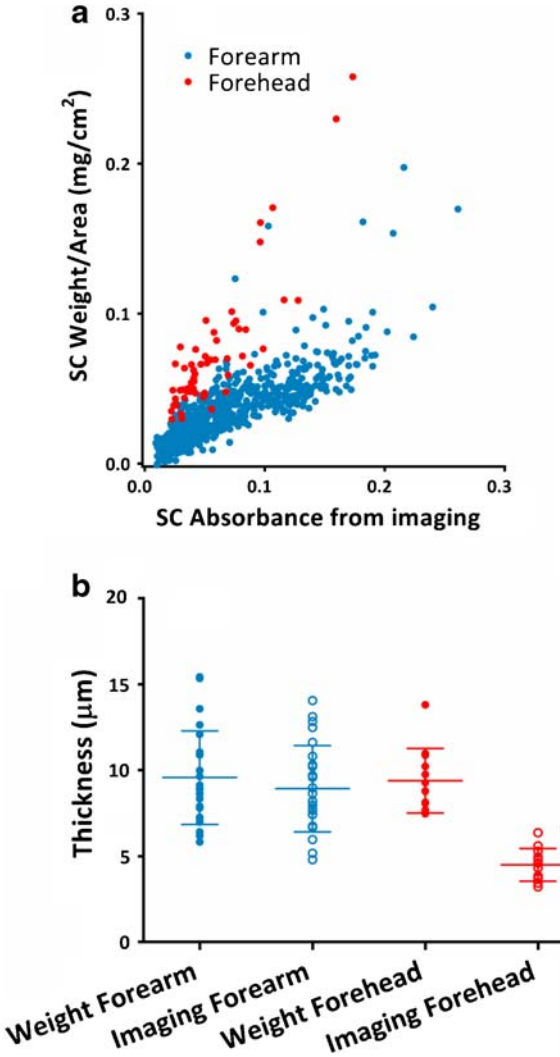

Fig. 2 (**a**) Correlation of SC quantification by gravimetric and imaging methods on the forearm (blue; $n=678$) and forehead (red; $n=59$). (**b**) Predicted SC thickness from gravimetric and imaging methods on forearm and forehead. The forehead SC thickness measured by imaging method is significantly different from all others ($P<0.0001$, 1-way ANOVA followed by Bonferroni's multiple comparison test).

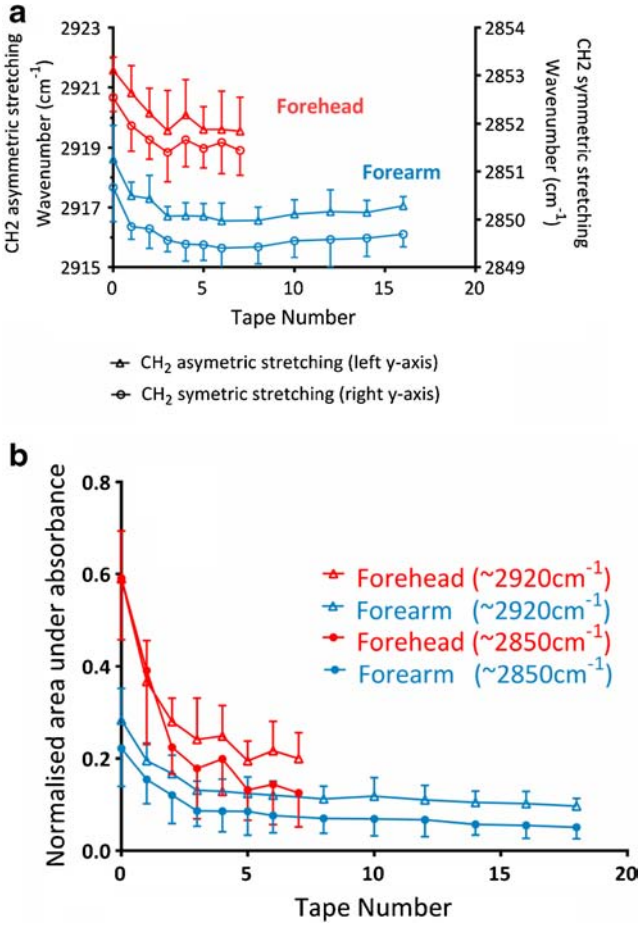

Fig. 3 (**a**) Peak CH_2 asymmetric (~2920 cm^{-1}) and symmetric (~2850 cm^{-1}) stretching frequencies as a function of tape-strip number (mean ± SD, $n=6$) on the forehead (*red*) and forearm (blue). The values before tape-stripping are significantly higher than those after (repeated measure one-way ANOVA followed by Bonferroni's multiple comparison test; $P<0.01$). (**b**) Normalised areas under the CH_2 asymmetric (~2920 cm^{-1}) and symmetric (~2850 cm^{-1}) stretching frequencies as a function of tape-strip number (mean ± SD, $n=6$) on the forehead (red) and forearm (*blue*). The values from the forehead are significantly higher that those from the forearm (repeated measure one-way ANOVA followed by Bonferroni's multiple comparison test; $P<0.01$).

measure one-way ANOVA followed by Bonferroni's Multiple Comparison Test, $p<0.01$). SC lipids on the forehead were much less ordered than those on the forearm (paired t-test, $p<0.0001$), consistent again with the enhanced levels of sebaceous material at this anatomic site.

The normalised areas under the CH_2 stretching absorbances were calculated as previously described (28), and a significantly higher level of lipids on the forehead, especially at the surface, was clear (Fig. 3b).

Significant correlations ($P<0.0001$) were evident between the spectroscopically estimated amounts of lipid on the forehead, deduced from both the asymmetric and symmetric CH_2 stretching absorbances, and the apparent weights of SC on the corresponding tape-strips (Spearman correlation coefficients of 0.62 and 0.65, respectively). The largest apparent weights corresponded completely with the highest lipid amounts and these data all came from measurements on the forehead. The important contribution of sebaceous lipids is strongly implicated once more, therefore (and the gravimetric approach to determine SC thickness at this anatomic site is clearly undermined).

Extraction of Amino-Acid-Derived Components of NMF

Twenty-one NMF components were successfully quantified. Other NMF components were detected but could not be quantified (methionine and taurine) while the chromatographic peaks of aspartic acid and asparagine either co-

eluted with unknown contaminants or suffered from severe ion suppression.

NMF Content in SC Determined by Tape-Stripping

Figure 4 illustrates the concentration profile, as a function of SC depth, for serine (an abundantly present), threonine (moderately abundant), phenylalanine (present at low levels) and glutamine (similarly, less abundant) on both the forehead (red) and forearm (blue). As stated above, high sebum secretion on the forehead results in higher apparent weights of SC removed and the gravimetric method was not used therefore to calculate NMF component concentrations. Weights of SC removed on each tape were determined using the imaging technique (and Eq. 1) and individual NMF component concentrations were then plotted in terms of mmol per kg of SC removed.

In most cases, NMF components present at high concentration (e.g., serine) in the skin had slightly higher levels on the forearm than on the forehead. For components of moderate

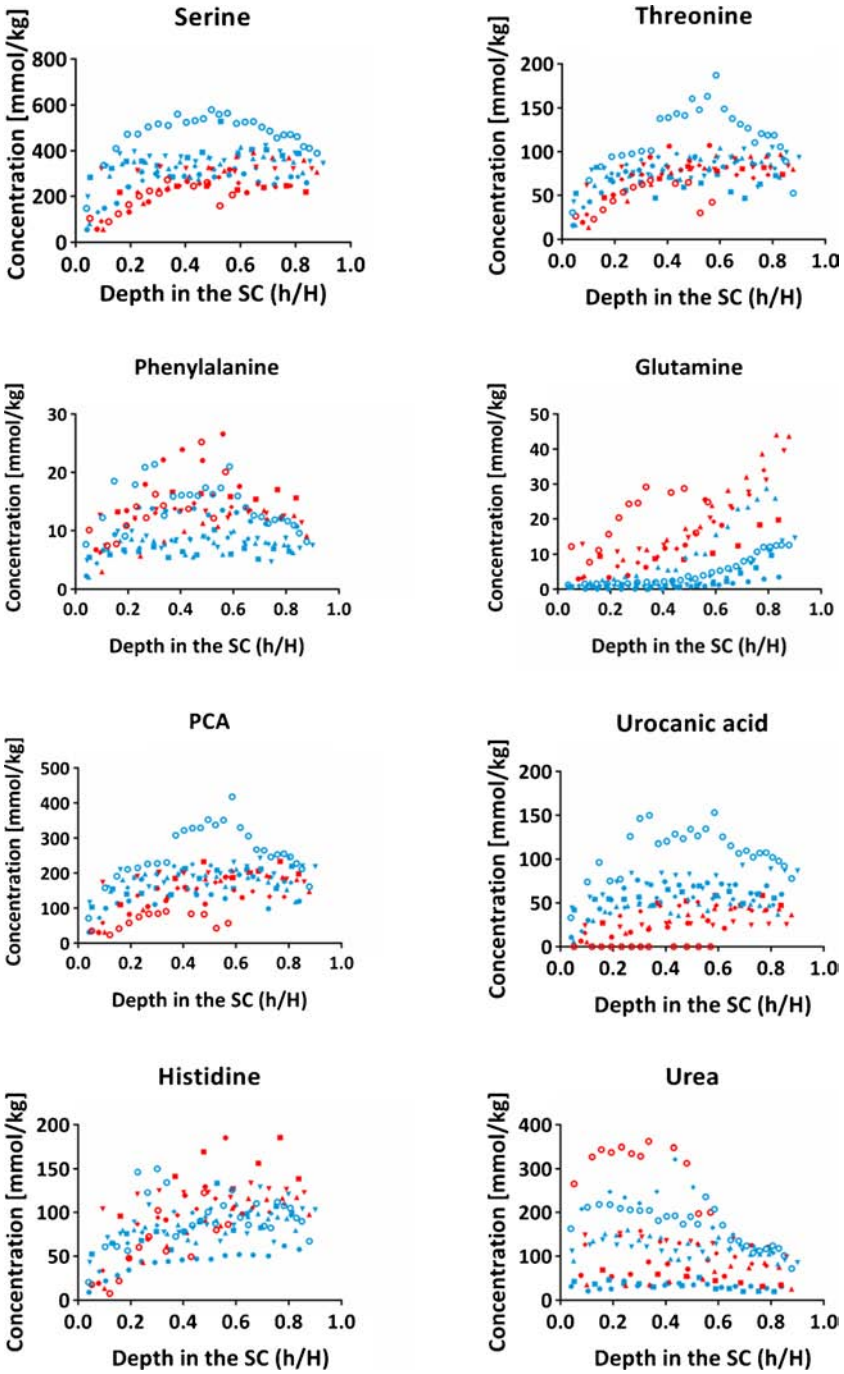

Fig. 4 Concentration profiles of serine, threonine, phenylalanine, glutamine, PCA, urocanic acid, histidine and urea as a function of normalised depth into the SC tape-stripped from the foreheads (*red*) and forearms (*blue*) of 6 human volunteers.

concentration (e.g., threonine), similar amounts were found at both sites. However, the NMF constituents present at low concentration appeared at modestly higher levels on the forehead, especially glutamine and glutamic acid. These higher amounts may reflect a shorter time available for their transformation into pyrrolidone carboxylic acid (PCA) in a thinner SC (5). Nevertheless, this transformation is still very efficient on the forehead, as shown by the relatively high amount of

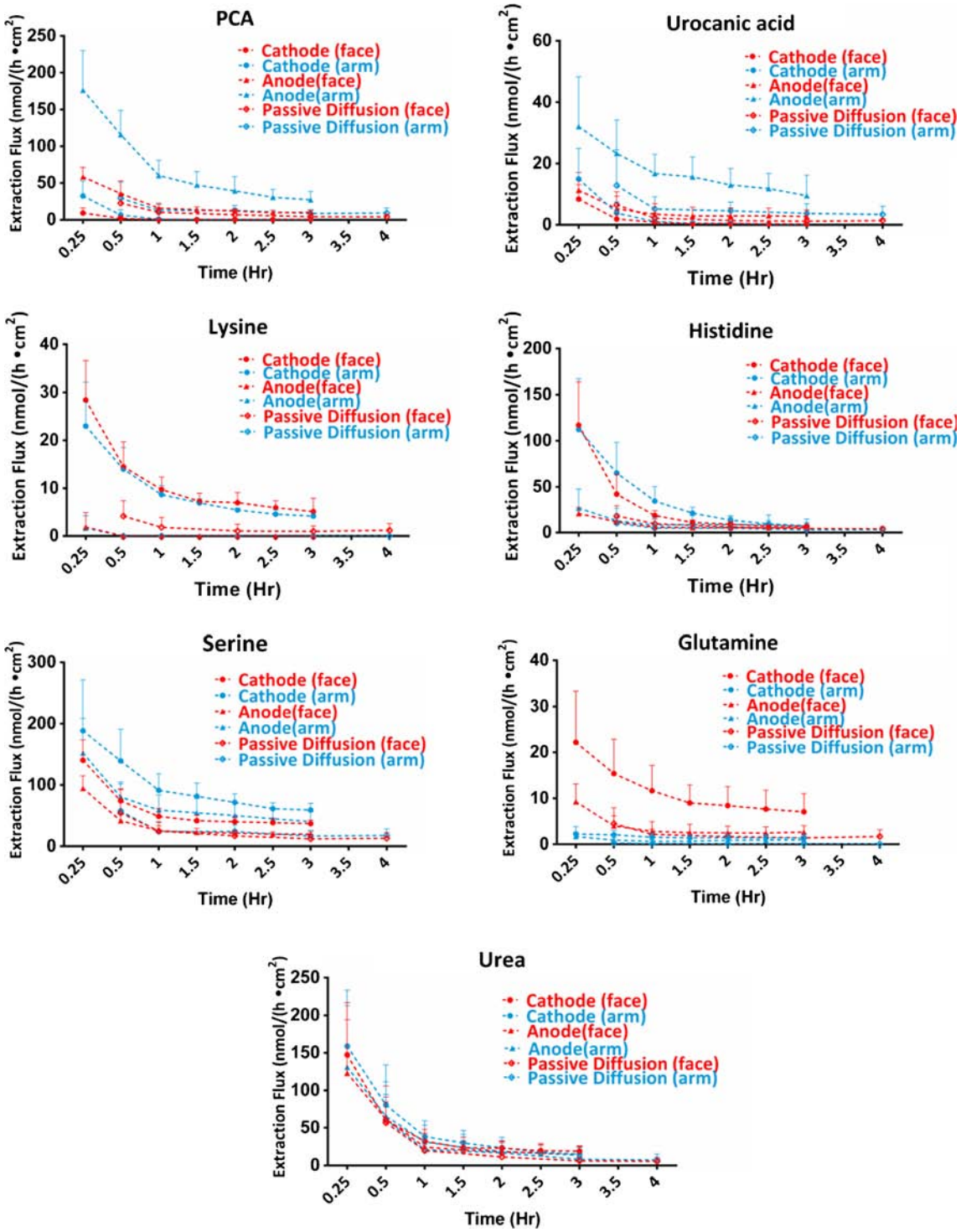

Fig. 5 Reverse iontophoretic and passive extraction fluxes (mean ± SD) of two acidic NMF components (PCA and urocanic acid), two basic constituents (lysine and histidine), two zwitterions (serine and glutamine) and an uncharged small molecule (urea) *in vivo* in human volunteers ($n = 6$) from forehead (*red*) and forearm (*blue*) skin as a function of time.

PCA present relative to glutamine. Because all the volunteers had healthy skin at both anatomic sites studied, wide differences in NMF levels were not expected.

Extraction by Reverse Iontophoresis and Passive Diffusion

Figure 5 presents examples of reverse iontophoretic and passive extraction of an acidic NMF component (PCA), a basic compound (lysine) and two zwitterions (serine and glutamine) from the forehead (red) and forearm (blue). The extraction fluxes of all NMF components showed a similar pattern on both skin sites: the initial flux was high and then decreased rapidly over the first hour before stabilising in the later 2 h.

The reverse iontophoretic and passive extraction of NMF components can be separated into three groups:

- Acidic compounds, negatively charged in solution at physiological pH, were extracted predominantly at the anode. The amounts extracted at the cathode were minimal and, in most cases, below the LOQ. As illustrated in Fig. 5, the extraction of PCA on the forearm in the first hour is much higher than that on the forehead, suggesting the presence of a much larger reservoir of PCA in forearm SC. It follows that the initial amounts of charged compounds extracted might be good indicators of levels in the SC.
- Extraction of compounds that are positively charged at physiological pH took place mainly at the cathode. The amounts detected at the anode and by passive diffusion were minimal in comparison. As lysine was found only in low amounts in the SC at both sites, the extraction profiles are very similar on the forehead and forearm.
- Zwitterions were extracted similarly to anode and cathode. Reverse iontophoresis only enhanced extraction by a modest extent, and little difference between forearm and forehead was observed. Glutamine was well extracted from forehead SC even though it was present at relatively low levels.

Origins of NMF Extracted

The amounts of NMF recovered by SC tape-stripping, passive extraction reverse iontophoresis are compared in Table I. With the exception of glutamic acid, all charged species were

Table I Cumulative Amounts (nmol/cm^2) of NMF Components Extracted in 3 h in SC Tape-Strips, by Passive Diffusion and by Reverse Iontophoresis (mean ± SD; $n = 6$)

	Tape-strips		Passive diffusion		Anode		Cathode	
	Forehead	Forearm	Forehead	Forearm	Forehead	Forearm	Forehead	Forearm
Charged compounds								
PCA	54 ± 24	151 ± 48	29 ± 14	45 ± 27	93 ± 62	176 ± 52	3.9 ± 4.5	11.0 ± 6.6
Urocanic acid	13 ± 4	40 ± 22	8.1 ± 5.0	15 ± 14	9.5 ± 10.2	66 ± 29	5.0 ± 4.4	15.9 ± 26.7
Glutamic acid	18 ± 5	15 ± 8	13 ± 6	2.9 ± 1.7	59 ± 9	36 ± 15	1.8 ± 1.4	0.42 ± 0.5
Histidine	37 ± 15	64 ± 18	29 ± 12	14 ± 7	18 ± 6	31 ± 31	66 ± 22	88 ± 29
Ornithine	6.1 ± 5.2	23 ± 16	6.4 ± 5.1	3.3 ± 3.6	2.2 ± 2.5	5.2 ± 6.1	28 ± 19	59 ± 38
Arginine	25 ± 14	37 ± 31	18 ± 11	5.3 ± 7.1	8.3 ± 6.2	7.6 ± 7.6	63 ± 21	52 ± 33
Lysine	7.8 ± 3.3	12 ± 6	6.2 ± 6.0	<LQL	0.3 ± 0.7	0.4 ± 0.6	28 ± 7	24 ± 4
Zwitterions and urea								
Serine	92 ± 33	283 ± 93	70 ± 35	86 ± 54	89 ± 15	202 ± 49	157 ± 31	264 ± 72
Glycine	44 ± 16	154 ± 46	37 ± 35	50 ± 30	46 ± 10	121 ± 31	73 ± 36	165 ± 49
Alanine	27 ± 7	98 ± 37	20 ± 8	31 ± 20	29 ± 8	66 ± 24	36 ± 15	69 ± 22
Threonine	26 ± 7	67 ± 22	16 ± 6	20 ± 12	17 ± 3	36 ± 13	26 ± 15	46 ± 14
Citruline	28 ± 5	71 ± 36	22 ± 14	22 ± 15	22 ± 11	38 ± 20	26 ± 13	46 ± 21
Valine	10 ± 2	26 ± 9	10 ± 4	9.6 ± 5.9	11 ± 2	16 ± 6	16 ± 5	17 ± 4
Proline	5.7 ± 1.7	18 ± 4	5.8 ± 2.7	5.6 ± 3.6	6.1 ± 2.3	12 ± 5	7.7 ± 3.7	12 ± 3
Tyrosine	7.9 ± 2.7	16 ± 5	5.6 ± 2.9	3.8 ± 2.4	8.1 ± 2.1	8.8 ± 5.0	10 ± 3	9.1 ± 2.4
Isoleucine	6.2 ± 0.9	14 ± 5	4.6 ± 2.4	3.2 ± 2.4	6.1 ± 1.7	7.7 ± 3.7	7.7 ± 2.4	7.1 ± 1.4
Leucine	8.1 ± 1.2	11 ± 5	7.4 ± 2.4	3.0 ± 1.5	8.7 ± 2.9	6.7 ± 3.0	10.9 ± 3.7	6.0 ± 1.3
Phenylalanine	5.1 ± 1.0	7.7 ± 3.5	4.5 ± 1.3	1.8 ± 1.3	5.3 ± 1.4	4.6 ± 1.9	6.3 ± 1.7	4.0 ± 0.8
Tryptophan	3.2 ± 1.0	6.6 ± 2.5	2.3 ± 1.3	1.6 ± 1.2	2.8 ± 1.0	3.4 ± 1.9	3.4 ± 1.0	2.8 ± 1.0
Glutamine	5.9 ± 2.0	3.3 ± 2.1	6.6 ± 3.8	0.4 ± 0.4	9.8 ± 5.4	2.9 ± 1.9	31 ± 13	4.6 ± 2.6
Urea	45 ± 27	93 ± 59	56 ± 35	66 ± 40	93 ± 62	105 ± 60	110 ± 37	122 ± 64

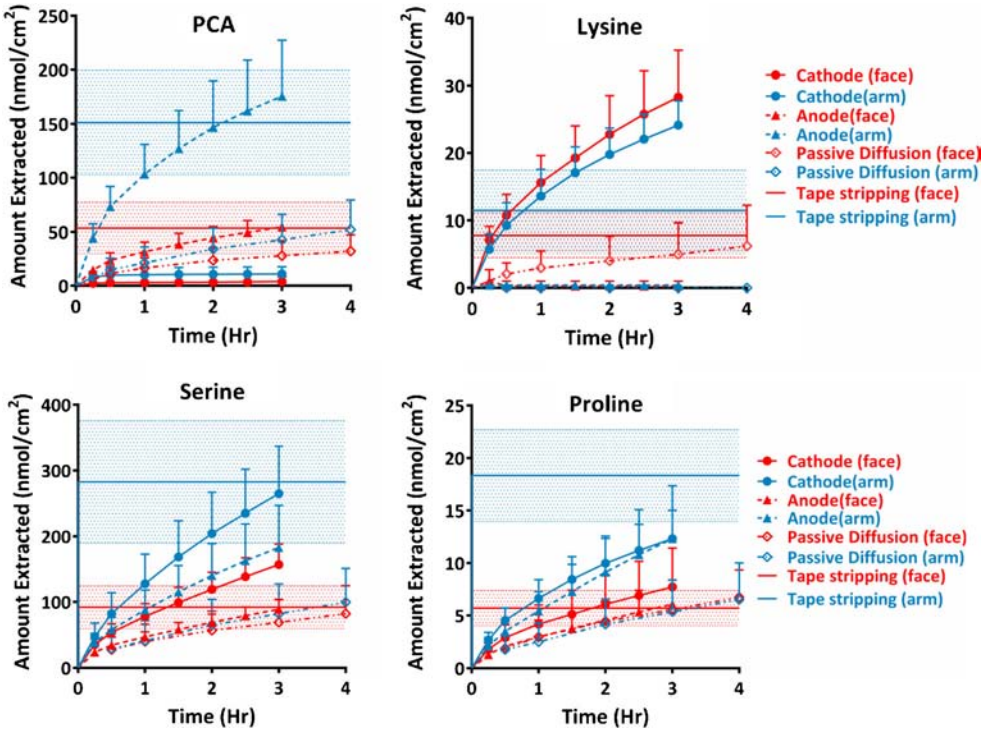

Fig. 6 Cumulative amounts ($n = 6$; mean ± SD) of PCA, lysine, serine and proline extracted by reverse iontophoresis and by passive diffusion as a function of time from the forehead (*red*) and forearm (*blue*). The average quantities in tape-stripped SC are shown for comparison by the solid horizontal lines, with the ±SD indicated by dashed lines.

detected in higher amounts in forearm SC removed by tape-stripping; however, passive extraction sometimes showed the opposite result; e.g., for lysine, passive extraction was clearly more efficient on the forehead. The higher amount found in tape-strips of forearm SC almost certainly reflects the greater thickness of the barrier and the 'volume' of tissue from which NMF is being extracted. By contrast, the more facile and efficient passive extraction from the forehead indicates the weaker permeability barrier and more rapid diffusion of small solutes therein.

Reverse iontophoresis is a powerful tool with which to extract charged molecules. By the end of 3 h, extraction to the preferred electrode was sampling analytes from beyond the SC (see data for PCA and lysine Fig. 6). The extent to which this is the case depends on the properties of the molecule and its concentration in the SC. For example, PCA is present in large quantity in the SC, and the time taken to deplete this compound is therefore much longer than that required for others, such as lysine. However, because the systemic concentration of PCA is very low (2.16±0.4 μM (30)), compared to that of essential amino acids (e.g., lysine, 100-300 μM (31)), the anodal extraction of PCA is essentially impossible to detect once the skin reservoir has been depleted. It follows that PCA extraction by reverse iontophoresis may be a sensible strategy with which to probe skin barrier function.

For the zwitterionic constituents of NMF (see data for serine and proline in Fig. 6), reverse iontophoresis could not deplete the amounts present in the 'SC reservoir' on the forearm by the end of 3 h; in contrast, extraction from forehead SC was almost complete. The quantities extracted by reverse iontophoresis were, on the whole, higher than those by passive diffusion, but not as dramatically different as seen for the charged compounds. Nevertheless, reverse iontophoresis improves the migration of the zwitterions significantly and higher extraction from the forearm has been observed.

Urea is a small molecule (60 Da), which readily permeates the skin. It is extracted efficiently by passive diffusion and, within 3 h, the amount in the SC has been just about depleted. However, as urea is also secreted from sweat onto the surface of the SC, the amount extracted shows considerable variability between subjects.

DISCUSSION

Minimally invasive bioengineering and biophysical techniques have been used to assess skin barrier function of the forearm and forehead of human volunteers *in vivo*. As a first step, a novel, recently developed imaging method has been compared to the traditional gravimetric approach with tape-stripping to quantify the stratum corneum. The new approach is fast, simple, and reproducible with an excellent signal-to-noise ratio. Correlation with infrared densitometry confirms that the imaging approach primarily evaluates the amount of SC via its protein content and it is not, therefore, subject to interference when attempting to quantify the barrier at skin sites, such as the forehead, where high levels of sebaceous lipids are found. The imaging approach also correlates with

the traditional gravimetric technique and thus offers a better standard method for SC quantification in the future.

Attenuated total reflectance, infrared spectroscopy (ATR-FTIR) was performed concomitantly with NMF extraction on both the forearm and forehead as two anatomic sites known to have clear differences in skin barrier function. Stratum corneum lipids on the forehead are more disordered, especially near the surface due to an extensive contribution from sebum. These results are fully consistent with published data (32), and the higher peak CH_2 stretching frequency observed on the forehead, even after extensive tape-stripping, attests to the "fluidisation" and increased conformational disorder (trans to gauche isomerisation) of lipids at this anatomic site (relative to the forearm) (26,33). A higher ratio of hexagonal-to-orthorhombic phase lipid on the forehead is suggested, therefore.

Filaggrin expression is essential for SC hydration, as it is the principal precursor protein for the amino-acid-derived components of the natural moisturizing factor (NMF), a complex mixture of low molecular weight humectants. Because of the small size and water solubility of these compounds, it was a reasonable hypothesis that reverse iontophoresis could be used for their minimally invasive extraction from the SC and this was indeed shown to be the case. The improvement achieved over passive extraction was influenced by molecular charge and the quantity of the specific NMF components within the SC. In fact, although a 4-h period of iontophoresis was insufficient to completely deplete this SC 'reservoir' of NMF in healthy human volunteers, those components, which are either highly charged or present only in minimal amounts (e.g. lysine), or that are found in the systemic circulation at very low levels (such as pyrrolidone carboxylic acid (PCA)), could be usefully extracted and quantified.

The concentrations of amino-acid derived NMF components at both sites are similar. However, forehead SC was found to be significantly thinner and generally contained a lower total absolute amount of NMF. Again, from the forehead, reverse iontophoresis efficiently extracted charged NMF components relative to passive extraction; however, only modest enhancement was achieved with zwitterionic species.

The concentration profiles of NMF components determined after SC tape-stripping (Fig. 4) agree with previous results (16) and with those reported using confocal Raman spectroscopy (6). The data for glutamine and pyrrolidone carboxylic acid (PCA), and for histidine and urocanic acid, merit consideration. It is noteworthy that, on the forehead, glutamine levels are higher compared to those on the forearm, whereas PCA concentrations are the other way round, suggesting that there is less time to achieve the biotransformation of the amino acid to PCA at the anatomic site where the SC is thinner. Similarly, the conversion of histidine to urocanic acid appears to be less efficient on the forehead, presumably for the same reason.

Of course, confocal Raman has also been shown capable of assessing SC thickness, hydration and lipid organisation, as well as semi-quantifying certain NMF constituents (16). However, this apparatus is expensive and not yet widely available and, by its very nature, cannot provide a direct read-out of absolute chemical concentrations as a function of depth into the skin (the loss of signal due to scattering and absorption making this impossible). In contrast, the less elegant tape-stripping approach, and the more modest reverse iontophoresis technique used in the research described here, offer direct quantification of most NMF components and the opportunity, therefore, to use this information as a biomarker for filaggrin expression and/or, more generally, skin "health".

Table II attempts to categorise NMF components based upon their concentration in the SC, their most suitable method of detection, and their potential to report on skin barrier function. The compounds in groups A and B are potentially

Table II Categorisation of NMF Constituents

Category	A	B	C	D	E
Concentration in SC (mmol/Kg)	>50	>50	>50	<50	<50
NMF constituents	Serine Glycine Alanine Threonine	Histidine PCA Urocanic acid	Citruline Ornithine Arginine Urea	Valine Proline Tyrosine Isoleucine Leucine Phenylalanine Tryptophan	Glutamine Glutamic acid Lysine
Potential skin "health" biomarker	+	+	−[a]	−[b]	±[c]
Preferred extraction method	Tape-stripping	Tape-stripping or reverse iontophoresis			Reverse iontophoresis

[a] Not recommended due to large inter-subject variability, although the sum (Arg + Cit + Orn) may be useful

[b] Not recommended due to low levels in SC

[c] Useful, perhaps, to monitor subcutaneous/systemic concentrations

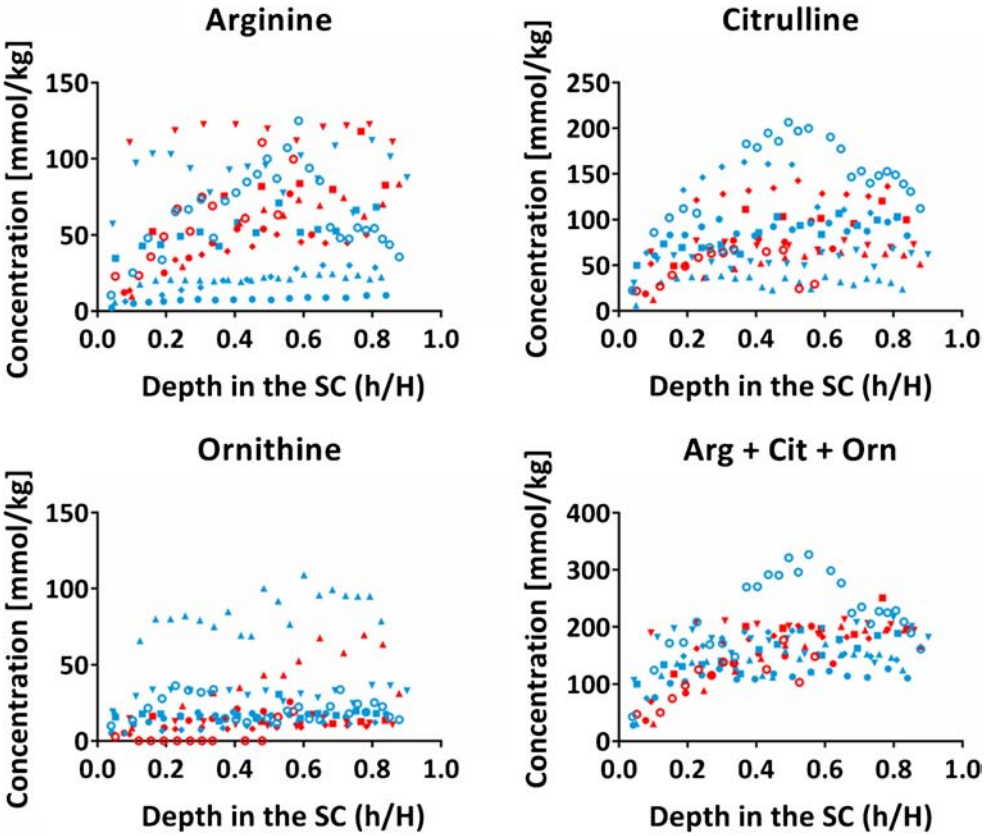

Fig. 7 Concentration profiles of arginine, citrulline, ornithine and the sum of {Arg + Cit + Orn} as a function of normalised depth into the SC tape-stripped from the forehead (*red*) and forearm (*blue*) of 6 human volunteers.

useful skin "health" biomarkers (and are unsurprisingly associated with filaggrin expression (4)), being present in relatively high concentration and readily extractable by tape-stripping, or by either tape-stripping or reverse iontophoresis, respectively. Electrotransport significantly enhances the extraction of the three NMF constituents in group B.

The components in group C are also present in the SC at high levels, but demonstrate a large inter-subject variability (Fig. 7). However, the sum of the three concentrations (Arg + Cit + Orn) is much more reproducible, and the collective distribution is quite similar to that of the individual compounds in groups A and B. It is known that ornithine is derived from the breakdown of arginine (by arginase-1), and that citrulline is the degradation product of arginine by nitric oxide synthase (NOS) (34) and peptidylarginine deiminases (PAD1 and PAD3) (35). As a result, it is possible that, while variability in enzyme activities between individuals may lead to marked differences in the individual levels of Arg, Cit and Orn, the sum of the amounts of the three compounds may be relatively constant across subjects as has in fact been observed. The extraction of urea also showed much variation, perhaps because it is additionally secreted in the sweat; this small molecule was as easily extracted by passive diffusion as by reverse iontophoresis.

The NMF components in group D were present in the SC at rather low levels which limited their usefulness as markers of skin barrier function. The group E constituents were also found in relatively low amounts within the SC, but were readily extractable from beneath the skin (sub-SC interstitial fluid) by reverse iontophoresis. While unlikely to be helpful in terms of the assessment of skin "health", there may be other monitoring applications of interest for molecules such as these.

CONCLUSIONS

The bioengineering and biophysical techniques employed in this research have been validated as useful and minimally invasive tools with which to characterise a number of important aspects of skin barrier function, including: SC thickness, lipid composition and conformational order, NMF composition and quantity. Furthermore, the metrics obtained are discriminatory between two anatomic sites, forearm and forehead, well known to differ in their barrier characteristics. It is now reasonable to envisage and design further research using the approaches described to examine and monitor changes in skin barrier "health" when the SC is either deliberately or pathologically undermined, and is then allowed to recover. Such is the focus of the next stage of this work.

ACKNOWLEDGMENTS AND DISCLOSURES

Quan Yang thanks the University of Bath for the award of a PhD studentship.

Disclaimer The opinions expressed in the paper are those of the authors alone and not those of MHRA.

REFERENCES

1. Rawlings A, Matts P. Stratum corneum moisturization at the molecular level : an update in relation to the dry skin cycle. J Invest Dermatol. 2005;124(6):1099–110.
2. Scott IR, Harding CR, Barrett JG. Histidine-rich protein of the keratohyalin granules: source of the free amino acids, urocanic acid and pyrrolidone carboxylic acid in the stratum corneum. Biochim Biophys Acta. 1982;719(1):110–7.
3. Rawlings A, Harding C. Moisturization and skin barrier function. Dermatol Ther. 2004;17(s1):43–8.
4. Kezic S, Kemperman P, Koster E, de Jongh C, Thio H, Campbell L, *et al.* Loss-of-function mutations in the filaggrin gene lead to reduced level of natural moisturizing factor in the stratum corneum. J Invest Dermatol. 2008;128(8):2117–9.
5. Barrett JG, Scott IR. Pyrrolidone carboxylic acid synthesis in guinea pig epidermis. J Invest Dermatol. 1983;81(2):122–4.
6. Caspers PJ, Lucassen GW, Carter EA, Bruining HA, Puppels GJ. In vivo confocal Raman microspectroscopy of the skin: noninvasive determination of molecular concentration profiles. J Invest Dermatol. 2001;116(3):434–42.
7. Muller S, Marenholz I, Lee Y, Sengler C, Zitnik S, Griffioen R, *et al.* Association of filaggrin loss-of-function-mutations with atopic dermatitis and asthma in the Early Treatment of the Atopic Child (ETAC) population. Pediatr Allergy Immunol. 2009;20(4):358–61.
8. Nomura T, Akiyama M, Sandilands A, Nemoto-Hasebe I, Sakai K, Nagasaki A, *et al.* Prevalent and rare mutations in the gene encoding filaggrin in Japanese patients with ichthyosis vulgaris and atopic dermatitis. J Invest Dermatol. 2009;129:1302–5.
9. Nemoto-Hasebe I, Akiyama M, Nomura T, Sandilands A, McLean WHI, Shimizu H. Clinical severity correlates with impaired barrier in filaggrin-related eczema. J Invest Dermatol. 2009;129(3):682–9.
10. Brown SJ, Irvine AD. Atopic eczema and the filaggrin story. Semin Cutan Med Surg. 2008;27(2):128–37.
11. Kezic S, Kammeyer A, Calkoen F, Fluhr JW, Bos JD. Natural moisturizing factor components in the stratum corneum as biomarkers of filaggrin genotype: evaluation of minimally invasive methods. Br J Dermatol. 2009;161(5):1098–104.
12. Horii I, Nakayama Y, Obata M, Tagami H. Stratum corneum hydration and amino acid content in xerotic skin. Br J Dermatol. 1989;121(5):587–92.
13. Takahashi M, Tezuka T. The content of free amino acids in the stratum corneum is increased in senile xerosis. Arch Dermatol Res. 2004;295(10):448–52.
14. Denda M, Hori J, Koyama J, Yoshida S, Nanba R, Takahashi M, *et al.* Stratum corneum sphingolipids and free amino acids in experimentally-induced scaly skin. Arch Dermatol Res. 1992;284 (6):363–7.
15. Sylvestre JP, Bouissou CC, Guy RH, Delgado-Charro MB. Extraction and quantification of amino acids in human stratum corneum in vivo. Br J Dermatol. 2010;163(3):458–65.
16. Sieg A, Jeanneret F, Fathi M, Hochstrasser D, Rudaz S, Veuthey J-L, *et al.* Extraction of amino acids by reverse iontophoresis in vivo. Eur J Pharm Biopharm. 2009;72(1):226–31.
17. Ya-Xian Z, Suetake T, Tagami H. Number of cell layers of the stratum corneum in normal skin – relationship to the anatomical location on the body, age, sex and physical parameters. Arch Dermatol Res. 1999;291(10):555–9.
18. Rougier A, Lotte C, Maibach HI. In vivo percutaneous penetration of some organic compounds related to anatomic site in humans: Predictive assessment by the stripping method. J Pharm Sci. 1987;76(6):451–4.
19. Machado M, Salgado TM, Hadgraft J, Lane ME. The relationship between transepidermal water loss and skin permeability. Int J Pharm. 2010;384(1–2):73–7.
20. Rougier A, Lotte C, Corcuff P, Maibach HI. Relationship between skin permeability and corneocyte size according to anatomic site, age, and sex in man. J Soc Cosmet Chem. 1988;39(1):15–26.
21. Harding C, Long S, Richardson J, Rogers J, Zhang Z, Bush A, *et al.* The cornified cell envelope: an important marker of stratum corneum maturation in healthy and dry skin. Int J Cosmet Sci. 2003;25(4):157–67.
22. Voegeli R, Rawlings A, Doppler S, Heiland J, Schreier T. Profiling of serine protease activities in human stratum corneum and detection of a stratum corneum tryptase-like enzyme. Int J Cosmet Sci. 2007;29 (3):191–200.
23. Russell LM, Guy RH. Novel imaging method to quantify stratum corneum in dermatopharmacokinetic studies: proof-of-concept with acyclovir formulations. Pharm Res. 2012;29(12):3362–72.
24. Russell LM, Guy RH. Novel imaging method to quantify stratum corneum in dermatopharmacokinetic studies. Pharm Res. 2012;29 (9):2389–97.
25. Mohammed D, Yang Q, Guy RH, Matts PJ, Hadgraft J, Lane ME. Comparison of gravimetric and spectroscopic approaches to quantify stratum corneum removed by tape-stripping. Eur J Pharm Biopharm. 2012;82(1):171–4.
26. Mendelsohn R, Flach CR, Moore DJ. Determination of molecular conformation and permeation in skin via IR spectroscopy, microscopy, and imaging. Biochim Biophys Acta. 2006;1758(7):923–33.
27. Kalia YN, Alberti I, Sekkat N, Curdy C, Naik A, Guy RH. Normalization of stratum corneum barrier function and transepidermal water loss in vivo. Pharm Res. 2000;17(9):1148–50.
28. Bommannan D, Potts RO, Guy RH. Examination of stratum corneum barrier function in vivo by infrared spectroscopy. J Investig Dermatol. 1990;95(4):403–8.
29. Russell LM, Wiedersberg S, Delgado-Charro MB. The determination of stratum corneum thickness An alternative approach. Eur J Pharm Biopharm. 2008;69(3):861–70.
30. Wolfersberger MG, Tabachnik J. Pyrrolidone carboxylic acid (pyroglutamic acid) in normal plasma. Cell Mol Life Sci. 1973;29 (3):346–7.
31. Kingsbury KJ, Kay L, Hjelm M. Contrasting plasma free amino acid patterns in elite athletes: association with fatigue and infection. Br J Sports Med. 1998;32(1):25–32.
32. Brancaleon L, Bamberg MP, Kollias N. Spectral differences between stratum corneum and sebaceous molecular components in the mid-IR. Appl Spectrosc. 2000;54(8):1175–82.
33. Gay CL, Guy RH, Golden GM, Mak VHW, Francoeur ML. Characterization of low-temperature (i.e., < 65 degrees C) lipid transitions in human stratum corneum. J Investig Dermatol. 1994;103(2):233–9.
34. Abeyakirthi S, Mowbray M, Van Overloop L, Wheatley P, Morris R, Declercq L, *et al.* Arginase enzyme is overactive in non-lesional psoriatic skin. Nitric Oxide. 2008;19(Supplement 1):35.
35. Chavanas S, Méchin M-C, Nachat R, Adoue V, Coudane F, Serre G, *et al.* Peptidylarginine deiminases and deimination in biology and pathology: relevance to skin homeostasis. J Dermatol Sci. 2006;44(2): 63–72.